Thermochimica Acta, 206 (1992) 187–201
Elsevier Science Publishers B.V., Amsterdam

Influence of sintering temperature and lead content on the formation of the high temperature superconducting phase in $Bi_{2-x}Pb_xSr_2Ca_2Cu_3O_y$

Micky Puri, Stephane Cuvier, John Bear and Larry Kevan

Department of Chemistry and Texas Center for Superconductivity, University of Houston, Houston, TX 77204-5641 (USA)

(Received 18 November 1991)

Abstract

The formation of the high temperature superconducting phase in $Bi_{2-x}Pb_xSr_2Ca_2Cu_3O_y$ ($x = 0$, 0.2, 0.4, 0.6, 0.8) with a superconducting transition temperature (T_c) near 110 K is studied as a function of sintering temperature and lead content. The optimum range of sintering temperature is based on differential thermal analysis (DTA) results. DTA shows two endothermic peaks near 1135 and 1155 K. The temperature difference between these two peaks varies with lead content and is maximum at $x = 0.4$. The $x = 0.4$ sample also shows the highest fraction of high T_c phase based on X-ray diffraction (XRD) and resistance measurements. Thus DTA, XRD and resistance measurements all independently support the $x = 0.4$ composition as having a unique response which seems characteristic of the high T_c phase. XRD and DTA results also suggest that the high T_c phase is formed by a reaction between the low T_c phase and the products of decomposition of Ca_2PbO_4 which is produced during the synthesis.

INTRODUCTION

The stabilization of the higher (about 110 K) superconducting transition temperature (T_c) phase $Bi_2Sr_2Ca_2Cu_3O_x$ (2223) in the Bi–Sr–Ca–Cu–O system relative to the lower (about 80 K) T_c phase $Bi_2Sr_2CaCu_2O_x$ (2212) has been the focus of numerous studies [1–47]. Different dopings or substitutions have been tried with some success. Thus far, the most efficient substituent seems to be lead oxide, though potassium [12] and praseodymium [13] also give a significant improvement in the amount and stability of the high T_c phase. Silver, when used as an additive with lead oxide, has been shown to sharpen the superconducting transition temperature [14,15]. Antimony when used as an additive with lead oxide, has also been reported to raise the transition temperature to about 130 K [16,17]. However, in lead-substituted 2223 superconductors, the solubility of anti-

Correspondence to: L. Kevan, Department of Chemistry and Texas Center for Superconductivity, University of Houston, Houston, TX 77204-5641, USA.

mony is very low and no increase in the transition temperature is observed [18]. It has also been suggested that lead and antimony partially substitute for bismuth and thereby promote the formation and stability of the high T_c phase [19]. Lead-free antimony-doped 2223 compounds are known to be nonsuperconductors [20].

Various explanations have been proposed to rationalize the role of lead oxide during the synthesis. It has been observed from differential thermal analysis (DTA) that the endothermic reaction peaks and also the melting point of lead-doped ceramics are shifted to lower temperatures as the lead ratio increases [21–23]. Therefore, PbO is suggested to be a flux assisting the formation of the high T_c phase or to act as a catalyst [21,22]. A strong dependence of the ratio of the high- and low-T_c phases in this system upon the lead content has been explained by competing processes between the action of PbO as a flux and the formation of Ca_2PbO_4 [21,24,25]. It has been suggested that there may be a competition between the growth of the 2223 phase, Ca_2CuO_3 and/or Pb_2CuO_4 [26]. It has also been proposed that the high T_c phase and $Bi_2Sr_2CuO_x$ are obtained from a disproportionation reaction of the low T_c phase [26].

The direct participation of lead atoms in the formation of the high T_c phase by substitution in the bismuth layers has been observed by high resolution analytical microscopy [28,29]. The resulting lead to bismuth ratio is close to 1.9 indicating a partial substitution of bismuth by lead [30]. In addition to the lead exchange in the bismuth layers, it is also reported that the bismuth sites are 40% strontium substituted [30]. The effect of this substitution is to stabilize the structure and facilitate its formation as a relatively pure phase [31].

The principal results of previous studies on this lead-doped system show that, like the lead-free system, the synthesis conditions and starting stoichiometry play an important role in the formation of the high T_c phase. Thus far, zero resistance has been achieved at temperatures close to 110 K, although magnetic susceptibility measurements mostly show the presence of another superconducting phase with a lower T_c. Contrary to the lead-free system, a synthesis with an initial stoichiometry close to $(Bi,Pb)_2Sr_2Ca_2Cu_3O_y$ results in the formation of the high T_c phase with the 2223 composition.

Stoichiometric variations of the lead to bismuth ratio between 10 and 30 mol% lead to superconducting materials with T_c from 90 to 110 K. Even if some discrepancies regarding the synthesis conditions remain, it appears that outside a lead ratio of 10–30 mol% a second superconducting phase with a lower T_c and Ca_2PbO_4 are formed [33,34]. Different optimum sintering temperatures seem to result in more of the high T_c phase which is preferentially formed for longer sintering times [35–39].

Here, the influence of the sintering temperature as well as lead content on the properties of the Bi–Pb–Sr–Ca–Cu–O system are studied by X-ray

diffraction, resistance and DTA measurements. DTA is shown to determine the optimum sintering temperature.

EXPERIMENTAL SECTION

The lead-substituted samples were prepared by grinding in an agate mortar appropriate amounts of PbO, Bi_2O_3, $CaCO_3$, $SrCO_3$ and CuO to constitute a $Bi_{2-x}Pb_xCa_2Sr_2Cu_3O_y$ stoichiometry ($x = 0$, 0.2, 0.4, 0.6 and 0.8). The powdered mixture is heated at 1063 K for 20 h in air, then reground and small pellets are pressed with a pressure of 11×10^6 kg m^{-2} (7 ton in.$^{-2}$) and sintered by heating in air at 1123, 1133, 1143 or 1153 K for 40 h. The samples were then reground, repelletized and sintered for an additional 40 h at each temperature. Each sample is denoted by its lead content, the temperature in kelvin at which the sintering step was performed and the sintering time in hours at this temperature. For example, PbO.4/1133/80 has a $Bi_{1.6}Pb_{0.4}Ca_2Sr_2Cu_3O_y$ initial stoichiometry and has been calcined at 1063 K for 20 h and sintered at 1133 K for 80 h in two 40 h steps.

Powder X-ray diffraction (XRD) was performed on a D-5000 Siemens diffractometer, using Cu K_α radiation with nickel filters at 30 kV and 25

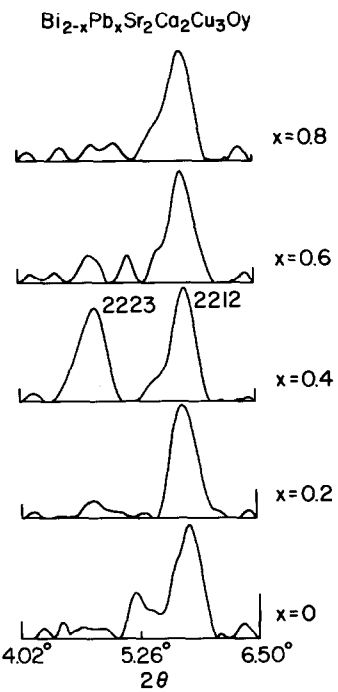

Fig. 1. XRD for $Bi_{2-x}Pb_xSr_2Ca_2Cu_3O_y$ samples as a function of x in the 2θ range 4–6.5°. All samples were sintered in air at 1143 K for 80 h.

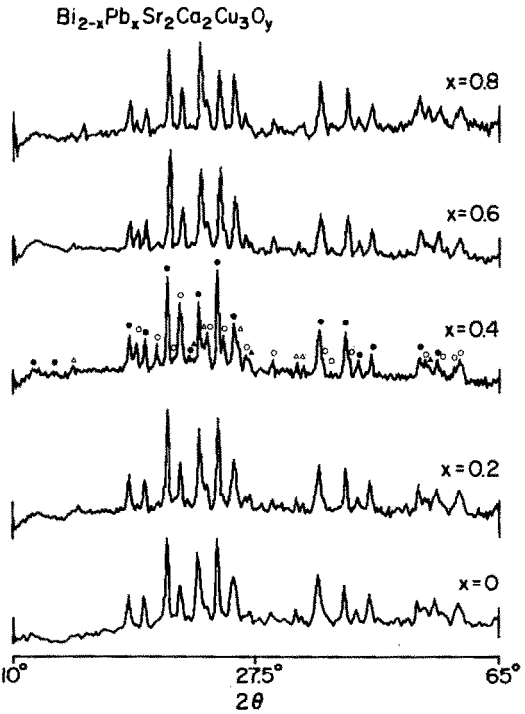

Fig. 2. XRD for $Bi_{2-x}Pb_xSr_2Ca_2Cu_3O_y$ samples as a function of x in the 2θ range 10–65°. Full circles, 2212 phase; open circles, 2223 phase; full triangle, Ca_2CuO_3; open triangle, Ca_2PbO_4, open square, PbO_2. All samples were sintered in air at 1143 K for 80 h.

mA. In the 2–10° range of 2θ a step size of 0.1 deg s^{-1} was used with 1 mm divergence and scatter slits and a receiving slit of 0.1 mm. For the 10–70° range of 2θ a step size of 0.03 deg s^{-1} was used with 1 mm divergence and scatter slits and a 0.2 mm receiving slit.

TABLE 1

Relative peak intensities of the 2212 and 2223 phases and certain impurity phases in the $Bi_{2-x}Pb_xSr_2Ca_2Cu_3O_y$ system sintered at 1143 K for 80 h [a]

x	Phase		Ca_2PbO_4	CaO_4	Ca_2CuO_3	PbO_2	Phase	
	2223 4.7 [b]	2212 5.7 [b]	17.8 [b]	46.4 [b]	36.8 [b]	59.7 [b]	2223 26.2 [b]	2212 27.5 [b]
0.0	5	100	0.0	–	13	–	5.7	100
0.2	14	100	0.8	3.4	15	7.9	6.3	100
0.4	84	100	1.8	4.2	17	9.2	24	100
0.6	24	100	7.2	4.6	12	15	8.7	100
0.8	14	100	19	6.4	9.2	19	7.1	100

[a] The relative changes are only comparable vertically.
[b] 2θ value in degrees.

The resistances were measured using a four point contact method. Platinum wires were connected to four small indium contacts pressed on a piece of pellet. An alternating current of 130 μA with a frequency of 17 Hz is generated in the sample and the voltage drop is detected by a lock-in amplifier.

DTA was performed using a Dupont 9900 thermal analyzer system. Samples were run in platinum boats at a heating rate of 10 K min^{-1} in an atmosphere of air.

RESULTS

XRD

The growth of the superconducting 2212 (80 K) and 2223 (110 K) phases was investigated as a function of lead doping and sintering temperature. Figures 1 and 2 show the X-ray powder diffraction pattern for $Bi_{2-x}Pb_xCa_2Sr_2Cu_3O_y$ ($x = 0$, 0.2, 0.4, 0.6 and 0.8) sintered at 1143 K in the 4–6.5° and 10–65° ranges of 2θ, respectively. Coexistence of the two main superconducting phases 2212 and 2223 is observed. These samples all show the dominant diffraction peaks that have been assigned to the 2223 phase ($2\theta = 4.7°$, 23.9°, 28.8°, 33.8°) and to the 2212 phase ($2\theta = 5.7°$, 23.2°, 27.5°) as well as peaks from Ca_2PbO_4, Ca_2CuO_3 and CaO_4 [20,26,41,42]. Trace amounts of $Bi_2Sr_2CuO_x$ are also observed.

From the intensity of the 4.7° peak assigned to the 2223 phase relative to the 5.7° peak assigned to the 2212 phase, the relative amount of the 2223 phase is found to be maximum for $x = 0.4$ (Table 1). A similar maxima is obtained on comparing the relative peak intensities at $2\theta = 26.2°$ (2223 phase) and at 27.5° (2212 phase). However since the two intensities are not

TABLE 2

Relative XRD peak intensities for the $Bi_{1.4}Pb_{0.6}Sr_2Ca_2Cu_3O_y$ system under various sintering conditions

Sample	Phase		Ca_2PbO_4	CaO_4	Ca_2CuO_3	PbO_2	Phase
	2223 4.7 [a]	2212 5.7 [a]	17.8 [a]	46.4 [a]	36.8 [a]	59.7 [a]	2212 27.5 [a]
Pb0.6/1123/40		100	28		12	6.9	100
Pb0.6/1123/80	5.4	100	17	4.9	8.0	14	100
Pb0.6/1133/40	9.1	100	18	6.1	10	14	100
Pb0.6/1133/80	17.3	100	11	4.6	6.8	6.6	100
Pb0.6/1143/40	19.0	100	10	2.9	7.5	6.7	100
Pb0.6/1143/80	38.4	100	7.2	2.0	6.6	8.9	100

[a] 2θ value in degrees.

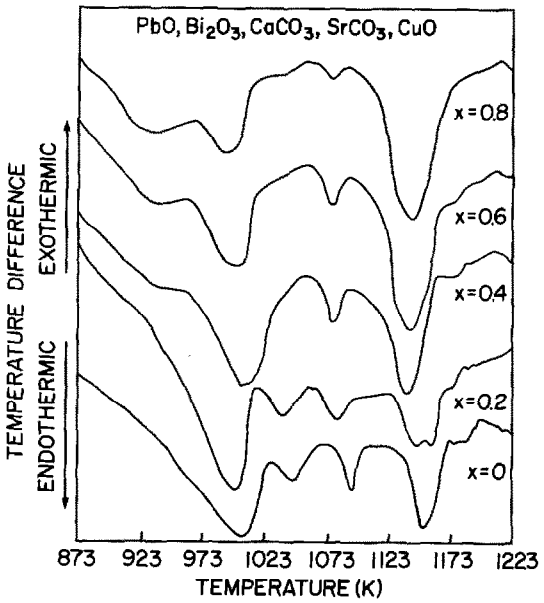

Fig. 3. DTA at a 10 K min^{-1} heating rate in air for ground mixtures of PbO, Bi_2O_3, $CaCO_3$, $SrCO_3$ and CuO in stoichiometric amounts needed to form $Bi_{2-x}Pb_xSr_2Ca_2Cu_3O_y$ samples.

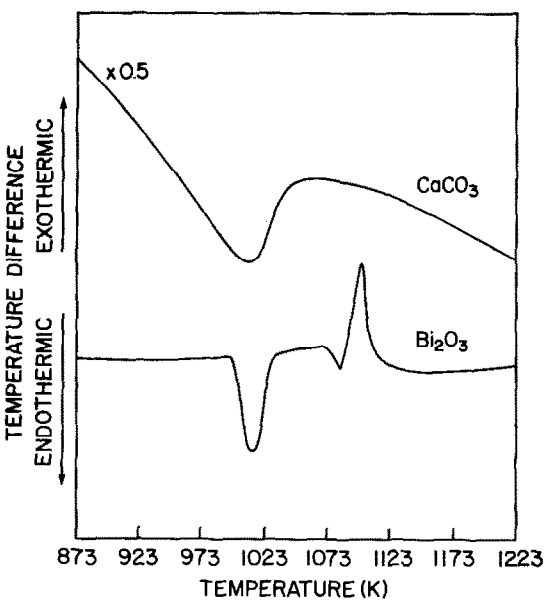

Fig. 4. DTA for Bi_2O_3 and $CaCO_3$ at a 10 K min^{-1} heating rate in air.

well resolved, the quantitative trends obtained with the intensities at low and high 2θ values are not similar. The peak at 7.2° is assigned to a semiconducting phase [24] and increases in intensity with increasing lead doping. For the undoped sample ($x = 0$) the peak at 5.23° could not be matched with an impurity phase. The formation of Ca_2PbO_4 ($2\theta = 17.8°$) [25] increases substantially with x while Ca_2CuO_3 ($2\theta = 36.8°$) [23] is detected in all the samples and decreases in intensity with increasing x.

A typical sample with initial stoichiometry of $Bi_{1.4}Pb_{0.6}Ca_2Sr_2Cu_3O_y$ was analyzed by XRD after each step in the synthesis. On the basis of the 4.7° relative peak intensity, it is evident that initially only the 2212 phase is formed (Table 2). The fraction of the 2223 phase increases with sintering time and temperature. The impurity phases detected are Ca_2PbO_4, Ca_2CuO_3, PbO_2 and CaO_4. With increasing sintering time and temperature, the Ca_2PbO_4 and Ca_2CuO_3 intensities decrease. The peak at 4.7° corresponding to the 2223 phase was found to grow in intensity only after long periods of sintering. With long sintering periods the high T_c phase may be formed from the low T_c phase by atomic rearrangement. Refined unit cell and structural parameters have shown that the 2223 phase is nonstoichiometric and that its composition changes with annealing temperature [42]. Adding lead to the Bi–Sr–Ca–Cu–O system increases the formation rate and the proportion of the high T_c phase possibly by facilitating the atomic rearrangement process. Our observations confirm

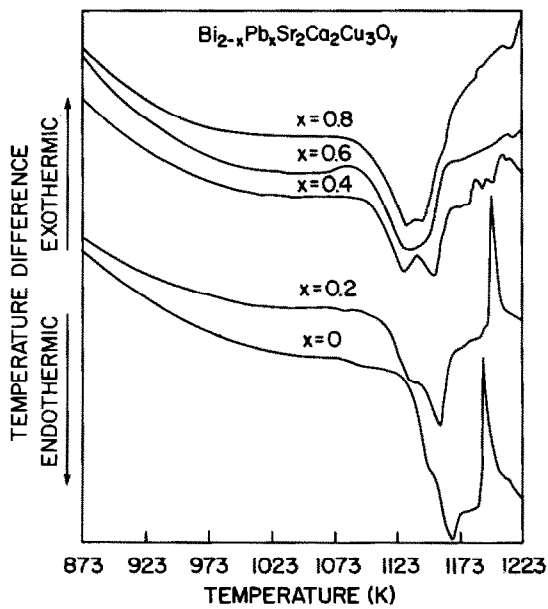

Fig. 5. DTA for $Bi_{2-x}Pb_xSr_2Ca_2Cu_3O_y$ samples at a 10 K min^{-1} heating rate in air. The samples were heated in air at 1063 K for 20 h but were not subsequently sintered.

TABLE 3

DTA endothermic peak temperatures as a function of x in $Bi_{2-x}Pb_xSr_2Ca_2Cu_3O_y$

x	Endothermic peak temperature (K)		ΔT (K)
	1	2	
0.0	1149	1166	17
0.2	1135	1157	22
0.4	1127	1153	26
0.6	1128	1147	20
0.8	1127	1143	16

that the low T_c phase is rather stable and it requires long periods of sintering to produce the high T_c phase from the low T_c phase [41].

DTA

Differential thermal analyses for the unreacted starting mixtures show for each stoichiometry a number of endothermic peaks which are generally shifted to lower temperatures as the lead content increases (Fig. 3). In order to attribute these different heat absorptions to a decomposition or a phase formation, Bi_2O_3, PbO, $CaCO_3$, $SrCO_3$ and CuO have been analyzed separately as well as in several mixtures of these oxides and carbonates. After each run the mixtures were found to have reacted with the walls of the platinum boats. The calcium carbonate to calcium oxide decomposition is easily detected in the mixtures (Fig. 3) and corresponds to the broad peak at 993–1013 K (Fig. 4). In addition, a phase transition occurs in the same temperature range for Bi_2O_3 (Fig. 3) which could be the cubic to

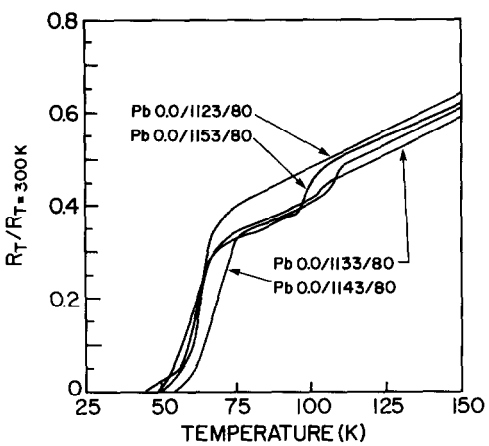

Fig. 6. Resistance versus temperature for samples Pb0/1123/80, Pb0/1133/80, Pb0/1143/80 and Pb0/1153/80.

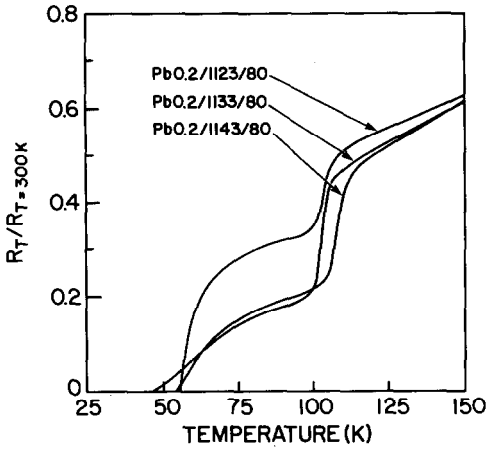

Fig. 7. Resistance versus temperature for samples Pb0.2/1123/80, Pb0.2/1133/80 and Pb0.2/1143/80.

rhombic transformation [44]. $SrCO_3$ is found to decompose above 1273 K and a phase transition or reduction to Cu_2O is also observed above 1273 K for CuO. The endothermic peak at 1223 K has been assigned to the melting point [46]. Therefore, the remaining unassigned endothermic peaks above about 1073 K are attributed to the formation of other unknown phases.

DTA was also performed for the samples heated in air at 1063 K for 20 h (Fig. 5). Increasing lead content changes the difference between the two overlapping endothermic peaks observed in the temperature range 1093–1193 K (Table 3). An interesting point is that the two peaks are best resolved at $x = 0.4$. For $x = 0$ and $x = 0.2$, a large exothermic peak is obtained around 1198 K (Fig. 5).

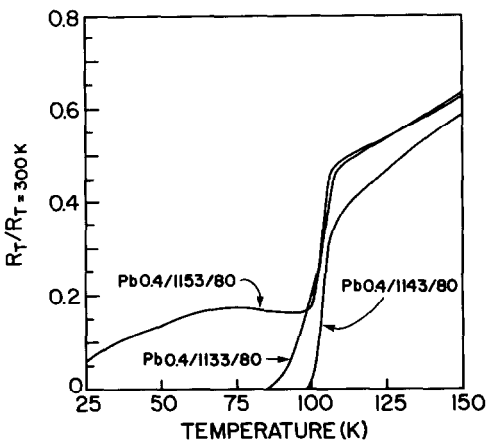

Fig. 8. Resistance versus temperature for samples Pb0.4/1133/80, Pb0.4/1143/80 and Pb0.4/1153/80.

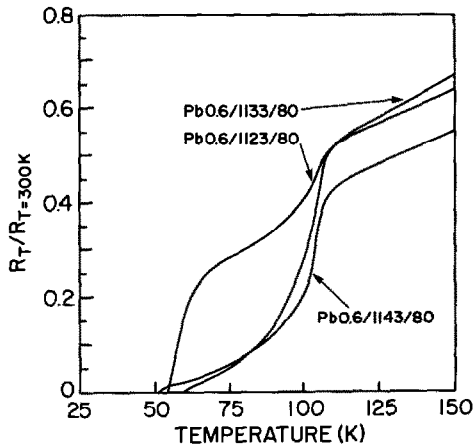

Fig. 9. Resistance versus temperature for samples Pb0.6/1123/80, Pb0.6/1133/80 and Pb0.6/1143/80.

Resistance measurements

The resistance versus temperature characteristics were measured for each sample. For sintering temperatures from 1123 to 1153 K, the lead-free samples show quite low high-T_c phase contents (Fig. 6). The sample sintered at 1123 K shows a resistance drop corresponding to the low T_c phase only. The resistance drop at 110 K increases with increasing sintering temperature but remains modest even at 1153 K. The temperature of zero resistance attainment and the commencement of the resistance drop for the high T_c phase is maximized in the sample that is sintered at 1143 K.

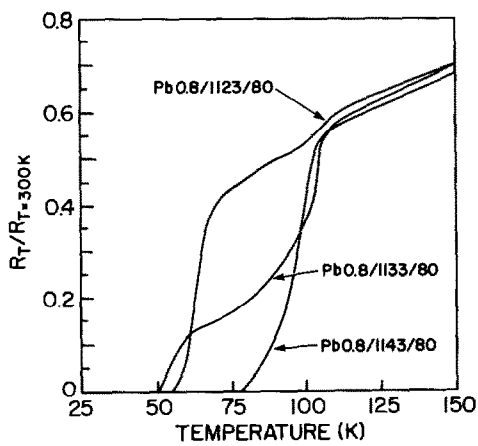

Fig. 10. Resistance versus temperature for samples Pb0.8/1123/80, Pb0.8/1133/80 and Pb0.8/1143/80.

Substitution of 10% of the bismuth by lead ($x = 0.2$) has a large effect on the development of the high T_c phase (Fig. 7). At a sintering temperature of 1133 K and above, a large resistance drop occurs near 100 K. The sample displaying a drop at the higher temperature of 110 K is obtained after sintering at 1143 K. However, the resistance does not drop to zero in this temperature range. For samples sintered at 1153 K, the resistance drop at 110 K was not significant and the resistance tail increased.

Further increase of the lead content (20% Pb substitution for $x = 0.4$) gives a material that shows zero resistance close to 100 K (Fig. 8). Above a sintering temperature of 1123 K, the second resistance drop close to 65 K slowly disappears and for 1143 K sintering, the sample attains zero resistance at 98 K. If the sample is sintered above 1153 K, the low T_c phase appears again.

For greater lead substitution ($x = 0.6$ and 0.8) a resistance drop at 110 K is observed but it does not drop to zero. The samples only reach zero resistance between 50 and 77 K (Figs. 9 and 10).

DISCUSSION

Though lead addition significantly raises the zero resistance in the Bi–Sr–Ca–Cu–O system, the synthesis conditions remain very critical. Even a modest temperature gradient inside the muffle furnace greatly affects the qualities of the superconductors as measured by resistance. A second batch of Pb0.4/1143/80 was prepared and pellets were placed in several crucibles at different positions in the same furnace but always at the same horizontal level. For some of the sintered pellets, zero resistance was obtained close to 100 K, but others displayed a large resistance drop at a lower temperature with zero resistance at 60 K. This extreme sensitivity to sintering temperature could explain why so many different optimum sintering conditions and diverse conclusions on the possible mechanism have been reported in the literature for this compound [21,24,27,28,33–37,45–48].

Nevertheless, these results are consistent with previous studies where it has been shown that outside a certain temperature range, a second superconducting phase with a lower T_c is produced [22,33,34,37,47,49,50]. Also, the optimum lead-to-bismuth substitution ratio agrees with the 10–30 mol% reported by other groups [21,23,28,34,36,45,47,48].

The high T_c phase is formed at a lower sintering temperature compared to the lead-free system which is consistent with the shift to lower temperatures of the heat evolution peaks in the DTA as the lead ratio increases (Table 3). The splitting of the two DTA peaks observed near 1143 K is most pronounced for the $Bi_{1.6}Pb_{0.4}Ca_2Sr_2Cu_3O_y$ stoichiometry and corresponds to the approximately 100 K zero resistance sample. X-Ray results also show the maximum fraction of the 2223 phase to be present for the

same stoichiometry (Table 1). The optimum synthesis temperature is considered to be located between these two endothermic peaks. It is reasonable to associate one of the two peaks to a new phase formation and the other to the partial melting of the sample [22] or to the formation of a liquid phase [27] which could act as a flux. DTA curves have been observed earlier for lead-doped $Bi_2Sr_2Ca_2Cu_3O_y$ phases [21,22,32,49]. However, all the endothermic peaks have not been assigned [32,49,51] and in some cases, only single peaks have been observed due to the melting of the sample [21]. In the $BiSrCaCu_2O_y$ system, we too observed a single DTA peak at 1170 K [52]. However, on careful evaluation, an additional weak peak at 1153 K is observed. This weak peak is most intense and best resolved at $x = 0.4$ which corresponds to the optimization of the 2223 phase. In Fig. 5, the sharp exothermic peak near 1200 K observed for $x = 0$ and $x = 0.2$ could be due to the reaction of the material with the walls of the platinum cup used for the DTA experiments.

The X-ray analysis in Table 1 suggests that the formation of Ca_2PbO_4 increases with lead content. Niva and co-workers have observed that this impurity is produced at temperatures lower than 1023 K during the synthesis process [25]. Ca_2PbO_4 decomposes around 1095 K to form CaO and a liquid phase. Since calcium is integrated into Ca_2PbO_4 below 1023 K, the formation of superconducting phases will proceed in a more calcium-deficient environment as the lead content increases. The growth of the lower T_c phase has been observed below the Ca_2PbO_4 decomposition temperature of 1095 K. This suggests that the high T_c phase may be formed by the action of CaO produced during the decomposition of Ca_2PbO_4 on the low T_c phase. The decrease in the X-ray diffraction intensity for the Ca_2PbO_4 phase with increasing sintering time and the simultaneous growth of the 2223 phase (Table 2) support this suggestion. It has also been suggested that there is a competition between the growth of the 2223 phase and Ca_2CuO_3 [40] rather than between the 2223 phase and Ca_2PbO_4 as suggested by others [21,24,25]. The observation that the X-ray peak corresponding to Ca_2CuO_3 ($2\theta = 36.8°$) is a maximum for the stoichiometry $x = 0.4$ does not agree with the Ca_2CuO_3 involvement even though its intensity decreases with increasing lead content (Table 1) and with increasing sintering time and temperature (Table 2).

An attempt has been made to identify the phase formation peaks seen by DTA above 1023 K (Fig. 3) in order to envisage a synthesis route involving intermediates formed from different combinations of the starting carbonates and oxides. Mixtures of Bi_2O_3, PbO, $SrCO_3$ $CaCO_3$ and CuO gave numerous endothermic peaks between 1023 and 1123 K, but too many effects such as eutectic formation or flux action are involved to definitely assign all peaks.

The resistance profiles reflect differences in the amounts of the high T_c superconducting phase. Zero resistance at 98 K means that at this tempera-

ture the current can percolate through a path constituted by a high T_c phase. This implies that there is a high probability of finding several islands of high T_c material in contact with each other. Although the resistance versus temperature measurements are not too quantitative, a sample with a two-step resistance drop such as Pb0/1153/80 (Fig. 6) is interpreted to contain less of the high T_c phase than one with a one-step resistance drop at 110 K such as Pb0.4/1143/80 (Fig. 8). Resistance measurements can fail to detect the presence of a minor quantity of a low T_c phase diluted in a higher T_c material. Therefore, although the electrical properties of the Bi–Sr–Ca–Cu–O system have been improved by lead addition, one must not rule out the presence of a lower T_c superconducting phase even though resistance measurements show a single resistance drop for certain samples.

CONCLUSIONS

Zero resistance close to 100 K has been achieved in the $Bi_{2-x}Sr_2Ca_2Cu_3O_y$ superconductor for $x = 0.4$. The resistance measurements indicate that the high T_c phase fraction is optimized for $x = 0.4$ in comparison with higher or lower x values. XRD results also show that the $x = 0.4$ composition has the greatest fraction of the high T_c superconducting phase. DTA and XRD results also suggest that the high T_c phase is formed by the action of Ca_2PbO_4 decomposition products on the low T_c phase. DTA shows two endothermic events near 1135 and 1155 K. The temperature difference between these two peaks appears to be dependent on the ratio of the high T_c to low T_c phases and is largest for $x = 0.4$. The optimum synthesis conditions for the high T_c phase are found to be close to 30 mol% lead substitution ($x = 0.4$) with a sintering temperature near 1143 K. The strong dependence of the zero resistance temperature upon the lead content could be due to the available amount of calcium left after the formation of the Ca_2PbO_4 intermediate phase.

ACKNOWLEDGMENT

This material is based upon work supported by the Texas Center for Superconductivity at the University of Houston under the prime grant MDA 972-88-G-0002 from the Defense Advanced Research Projects Agency and the State of Texas.

REFERENCES

1 S.A. Sunshine, L.F. Siegrist, D.W. Scheemeyer, R.J. Murphy, R.J. Cava, B. Batlogg, R.B. van Dover, R.M. Fleming, S.H. Glarum, S. Nakahara, R. Farrow, J.J. Krajewski, S.M. Zakura, J.V. Waszaczak, J.H. Marshall, P. Marsh, L.W. Rupp, Jr. and W.F. Peck. Phys. Rev. B, 38 (1988) 893.
2 J.S. Luo, D. Michel and J.P. Chevalier, Appl. Phys. Lett., 55 (1989) 1448.

3 Y. Takeda, R. Kanno, F. Tanigawa, O. Yamamoto, Y. Ikeda and M. Takano, Physica C, 159 (1989) 789.
4 R.A. Mohan Ram, P.S. Kobiela, W.P. Kirk and A.J. Clearfield, J. Solid State Chem., 83 (1989) 214.
5 H. Nobumasa, T. Arima, K. Shimitsu, Y. Otsuka, Y. Murata and T. Kawai, Jpn. J. Appl. Phys., 28 (1989) L57.
6 T. Komatsu, R. Sato, K. Matusita and T. Yamashita, Appl. Phys. Lett., 54 (1989) 1169.
7 T. Komatsu, R. Sato, C. Hirose, K. Matusita and T. Yamashita, Jpn. J. Appl. Phys., 27 (1988) L2293.
8 O. Smrckova, D. Sykorova, L. Smrcka and P. Vaseck, Phys. Status Solidi, 111 (1989) K77.
9 Y. Nishi, S. Moriya and T. Manabe, J. Appl. Phys., 65 (1989) 2389.
10 N. Murayama, M. Awano and E. Sudo, Jpn. J. Appl. Phys., 27 (1988) L2280.
11 P.V.P.S.S. Sastry, I.K. Gopalakrishnan, J.V. Yakhmi and R.M. Iver, Physica C, 157 (1989) 491.
12 T. Honda, T. Wada, M. Sakai, N. Miyajima, N. Nishikawa, S. Uchida, K. Uchinokura and S. Tanaka, Jpn. J. Appl. Phys., 27 (1988) L545.
13 S. Geller and K.-Y. Wu, Appl. Phys. Lett., 54 (1989) 669.
14 W. Gao, S.C. Li, D.A. Rudman, G.J. Yurek and J.B.V. Sandev, Physica C, 161 (1989) 71.
15 H.K. Liu, S.X. Dou, N. Savvides, T.P. Zhou, N.X. Tan, A.J. Bourdillon, M. Kviz and C.C. Sorrell, Physica C, 157 (1989) 93.
16 P.V.S.S. Sastry, I.V. Yakhmi and R.M. Iyer, Solid State Commun., 71 (1989) 935.
17 M.R. Chandrachood, I.S. Mulla and A.P.B. Sinha, Appl. Phys. Lett., 55 (1989) 1472.
18 B. Dabrowski, D.R. Richards, D.G. Hinks, R.H. Hannon, W. Peng, H. Lee, A.P. Genis, V.I. Melim and C.W. Kimball, Physica C, 160 (1989) 281.
19 M. Pissas and D. Niarchos, Physica C, 157 (1989) 643.
20 L. Hoongbao, Z. Xiaonong, C. Yaozu, Z. Guien, Y. Ruan, C. Zhajia, and Z. Yuheng, Physica C, 156 (1988) 804.
21 A. Oota, A. Kirihigashi, Y. Sasaki and K. Ohba, Jpn. J. Appl. Phys., 27 (1988) L2239.
22 T. Hatano, K. Aota, S. Ikeda, K. Nakamura and K. Ogawa, Jpn. J. Appl. Phys., 27 (1988) L2050.
23 M. Mizuno, H. Endo, J. Tsuchiya, N. Kljama, A. Sumiyama and Y. Oguri, Jpn. J. Appl. Phys., 27 (1988) L1225.
24 S. Koyama, U. Endo and T. Kawai, Jpn. J. Appl. Phys., 27 (1988) L1861.
25 T. Uzumaki, K. Yamanaka, N. Kamehara and K. Niva, Jpn. J. Appl. Phys., 28 (1989) L75.
26 C.Y. Yang, J.G. Wen, Y.F. Yan and K.K. Fung, Physica C, 160 (1989) 161.
27 N. Kijima, H. Endo, J. Tsuchiya, A. Sumiyama, M. Mutsuno and Y. Oguri, Jpn. J. Appl. Phys., 27 (1988) L1852.
28 U. Endo, S. Koyama and T. Kawai, Jpn. J. Appl. Phys., 28 (1989) L190.
29 M.P. Bansal and D.E. Farrell, Appl. Phys. Lett., 55 (1989) 1572.
30 T. Ishida, Jpn. J. Appl. Phys., 28 (1989) L197.
31 T. Nagashima, K. Watanabe, M. Watahiki and Y. Fukai, Jpn. J. Appl. Phys., 28 (1989) L183.
32 M. Mizuno, H. Endo, T. Tsuchiya, N. Kijima, A. Sumiyama and Y. Oguri, Jpn. J. Appl. Phys., 27 (1988) L1225.
33 A. Kikuchi, M. Matsuda, M. Takata, M. Ishii, T. Yamashita and H. Koinuma, Jpn. J. Appl. Phys., 27 (1988) L2300.
34 H.K. Liu, S.X. Dou, N. Savvides, J.P. Zhou, N.X. Tan, A.J. Bourdillon, M. Kviz and C.C. Sorrell, Physica C, 157 (1989) 93.
35 C.J. Kim, C.K. Rhee, H.G. Lee, C.T. Lee, J.-T. Kang and D.Y. Won, Jpn. J. Appl. Phys., 28 (1989) L45.

36 S.-I. Narumi, H. Ohtsu, I. Iguchi and R. Yoshizaki, Jpn. J. Appl. Phys., 28 (1989) L27.
37 H.G. Lee, C.J. Kim, K.H. Lee and D.Y. Won, Appl. Phys. Lett., 54 (1989) 391.
38 T. Takabatake, W. Ye, S. Orimo, H. Kawanaka, H. Fujii, H. Sasakura, and S. Minamigawa, Physica C, 127 (1989) 263.
39 H. Guchang, W. Yugui, W. Jinsong, W. Nanlin and J. Xinping, Solid State Commun., 29 (1989) 543.
40 B.W. Statt, Z. Wang, M.J.G. Lee, J.V. Yakhmi, P.C. De Camargo, J.F. Major and J.W. Rutter, Physica C, 156 (1988) 251.
41 M. Onoda, A. Yamato, E.T. Muromachi and S. Takekawa, Jpn. J. Appl. Phys., 27 (1988) 833.
42 W.C. Cabrera and W. Göpel, Physica C, 161 (1989) 373.
43 H.W. Zandbergen, K. Huang, M.J.V. Menken, J.N. Li, K. Kadowaki, A.A. Menovsky, G. van Tendelou and S. Amelinckx, Nature, 332 (1988) 620.
44 R.C. Weast and M.J. Astle, CRC Handbook of Chemistry and Physics, 62nd Edn., Chemical Rubber Co., Boca Raton, FL, 1981–1982, p. B-73.
45 A. Ono, Jpn. J. Appl. Phys., 28 (1989) L54.
46 Y. Ibara, H. Nasu, T. Imura and Y. Osaka, Jpn. J. Appl. Phys., 28 (1989) L37.
47 S.M. Green, C. Jiang, M. Mei, H.L. Luo and C. Politis, personal communication, 1988.
48 B. Zhu, L. Lei, S.L. Yuan, S.B. Tang, W. Wang, G.G. Zheng, W.Y. Guan and J.Q. Zheng, Physica C, 157 (1989) 370.
49 R. Sato, T. Komatsu, K. Matushita and T. Yamashita, Jpn. J. Appl. Phys., 28 (198) 583.
50 A. Ono, Jpn. J. Appl. Phys., 27 (1988) L2276.
51 L. Pierre, D. Morin, J. Schneck, J.C. Toledano, J. Primot, C. Daguet, F. Glas, J. Etrillard and H. Savary, Solid State Commun., 69 (1989) 499.
52 S. Cuvier, M. Puri, J. Bear and L. Kevan, J. Phys. Chem., 94 (1990) 3864.